IEEE Access
Multidisciplinary | Rapid Review | Open Access Journal

Received October 25, 2020, accepted November 20, 2020, date of publication November 26, 2020,
date of current version December 14, 2020.

*Digital Object Identifier 10.1109/ACCESS.2020.3040869*

# Optimal Control Strategy to Maximize the Performance of Hybrid Energy Storage System for Electric Vehicle Considering Topography Information

**TAHA SADEQ[1], (Member, IEEE), CHEW KUEW WAI[1], (Senior Member, IEEE), EZRA MORRIS[1], QAZWAN A. TARBOSH[2,3], (Member, IEEE), AND ÖMER AYDOĞDU[3]**

[1]Lee Kong Chian Faculty of Engineering and Science, Universiti Tunku Abdul Rahman, Sungai Long Campus, Selangor 43000, Malaysia
[2]Faculty of Electrical and Electronic Engineering, Selçuk University, 42130 Konya, Turkey
[3]Faculty of Engineering and Natural Sciences, Konya Technical University, 42130 Konya, Turkey

Corresponding author: Taha Sadeq (eng.tahasadeq@1utar.my)

This work was supported by Universiti Tunku Abdul Rahma Research Fund (UTARRF) Project No IPSR/RMC/UTARRF/2015-C1/C05 and KL Automation Engineering Sdn Bhd.

**ABSTRACT** This research designed an energy management system involving a battery-supercapacitor Hybrid Energy Storage System (HESS) for electric vehicles (EV). The objective is to improve the performance of the HESS by combining battery and supercapacitor features, accounting for topographical information to guarantee continuous hybridization during the drive cycle. Contour Positioning System (CPS) was used to determine the slope of the rode travelled by the vehicle. Two adaptive algorithms were designed for a rule-based controller to control the energy shared between the battery and the supercapacitor; an optimal adaptive controller and fuzzy adaptive controller. The HESS model, electric vehicle and controllers were tested using MATLAB/Simulink with three real drive cycles, namely, uphill, downhill and city tour, in three different speeds 50Km/h, 60Km/h and 70 Km/h. The results proved the controllers managed to extend battery life-cycle by reducing the stress on the battery for the drive cycles. The results were compared in terms of energy consumption for the optimal adaptive rule-based controller and fuzzy adaptive rule-based controller. The optimal adaptive rule-based controller guaranteed the HESS was able to operate continuously and extend the number of drive cycles in a wide range of speeds and road slopes.

**INDEX TERMS** Electric vehicles, energy storage, energy management, navigation.

## I. INTRODUCTION

The large interest surrounding Energy Storage Systems (ESSs) is motivated by the need to employ renewable energy resources instead of relying on fossil fuels. This need is related to two main concerns: the depletion in petroleum reservoirs and the threat of global warming. The needs to reduce air pollution and harmful emissions by conventional vehicles have promoted the development of electric vehicles (EVs). EVs remain to face issues that need to be resolved [1]–[3]. Batteries are among the most common energy storage devices, and they represent a large promise for clean energy [4]. Limited life-time and low power density are the main defects in Pure Battery Electric Vehicles (PBEVs). Hybrid energy storage system (HESS) is a practical solution that can be implemented for EV applications [5]–[7]. HESS is a combination of two different types or more of energy storage devices such as batteries, fuel cells, flywheels or supercapacitors. In HESS, the main storage device with high energy density such as batteries or fuel cells are used to provide a constant power load, while an auxiliary storage device with a high power density such as supercapacitors or flywheels is used to provide a fast dynamic response for load power change [8], [9]. The driving performance and cost of EVs essentially rely on the efficiency of the ESS and its capability, which can deliver a large amount of energy and respond

The associate editor coordinating the review of this manuscript and approving it for publication was Fabio Massaro.

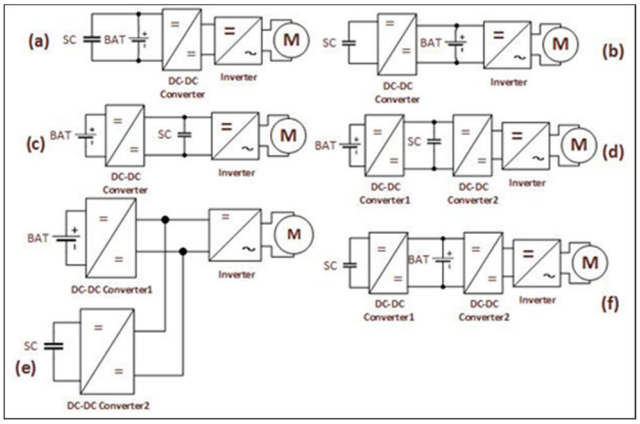


**FIGURE 1.** Common HESS architectures [11].

quickly to load demands [10]. This research incorporated a battery-supercapacitor HESS in an EV. Batteries remain the main energy storage device due to their high energy density. On the other hand, a supercapacitor has low energy density but high power density. The supercapacitor possesses unique properties that can complement other energy storage technologies. Generally, HESS is designed by interfacing the supercapacitor and battery via a bidirectional DC-DC converter to take advantage of the two, and in turn mitigate their limitations. Among the primary challenges in HESS design is assessing the configuration of the supercapacitor and battery with the DC bus. Many topologies for battery-supercapacitor interfaces have been attempted, each with its own advantages and disadvantages. Numerous studies in the literature have attempted to design battery-supercapacitor hybrid energy storage systems for EVs, with various topologies to interface between the battery and the supercapacitor [10]–[13]. Figure 1 illustrates different topologies of HESS. Furthermore, different types of bidirectional DC-DC converters have been used in an HESS for EV applications [14]. Among the most popular topologies is the semi-active HESS shown in Figure 1(b). Here, the DC-DC converter is used to control the power flow from the supercapacitor to the DC bus, and the system will not be affected by failure of the DC-DC converter.

A new topology to connect the battery and supercapacitor was investigated in [13], with the aim of reducing the overall size of the DC-DC converter in the HESS. The load in the HESS was controlled using four different modes. The simulation and experimental results showed improved performance of the proposed HESS. On the other hand, managing the power flow between the battery and supercapacitor in HESS remains a critical challenge. The energy management control scheme used to control the semi-active topology of the HESS, taking into account the regenerative energy of the electric vehicle, was presented in [15]–[17]. Furthermore, a fuzzy logic controller was used to split the load power between the battery and supercapacitors of HESS in [18]. The output of the fuzzy logic control affected the power for the battery and the supercapacitor, while the other two controllers drove the two DC-DC converters in the HESS. The high-precision digital elevation model [19] was used to measure the elevation of the road considered. Another work investigated a new energy management system for HESS for six standard drive cycles using a neural network [20]. The characteristic parameters were taken in real-time from the different drive cycles by the using slide time window to determine the load distributed components between the battery and supercapacitor. Other researchers attempted to improve the HESS and improve battery life in the EVs by formulating real-time energy problems. This helped to determine the optimal current split point between the battery and supercapacitor. A cost objective function was derived to minimize the battery current variations and amplitude, and reduce the error between the supercapacitor current and the reference current. A neural network-based strategy was used to split the load current between the battery and supercapacitor [21]. In [22], the researcher designed a fuzzy logic controller to manage the power distributed between the battery and supercapacitor. The total vehicle load demand, supercapacitor SOC and battery SOC were used as the controller's input. The ADVISOR platform was used to implement the model vehicle's control strategy. Another study compared the responses of three different control schemes to control a semi-active HESS in [23]. The main contribution was to improve vehicle performance by including an auxiliary ESS to support the main ESS. The system was tested via a simulation and experiment involving a real drive cycle for an EV model. It showed that a simple control can produce high performance. A more complex control scheme was designed to split the load power between the battery and supercapacitor to increase the efficiency of the HESS and overall battery life in [24]. The predictive controller was used to manipulate the duty cycle of the DC-DC converter to control the current of the supercapacitor during operations. Furthermore, the predictive controller reduced the frequent variation of battery load in the EV's HESS. A non-uniform sampling time approach was investigated in [25]. An adaptive power split strategy was used to split the load between the battery and the supercapacitor in the HESS for EVs in [26]. The controller drove the interleaved DC-DC converter in the semi-active HESS, and the Zero Voltage Switching method minimized the switching losses in the converter. The system was evaluated over four drive cycles in an EV. A new control strategy was proposed in [27] based on driving pattern recognition. The driving cycle was classified into different patterns based on the historical driving data. An adaptive wavelet transform was used to assign the high power demand to the supercapacitor, while the low frequency power demand was supplied by a battery. This strategy was implemented in a standard drive cycle and decreased the maximum charge/discharge current of the battery, improved the battery lifetime, and extended the vehicle range. A Markov chain method cooperated with a Monte Carlo method to propose a stochastic model from the history of the driving cycle in [28]. The predictive drive cycle was used to update the equivalent consumption minimization strategy in real-time to manage the energy flow in the HEV successfully.

The control strategy was implemented to drive the switching bi-directional buck-boost converter for vehicles- to-grid systems [29]. A state-space averaging approach was used to test the system stability. The controller considered the SOC of HESS to regulate the power flow in the system. The experimental results for laboratory prototypes were presented to verify the design. A real-time control strategy based on a Lyapunov-based nonlinear approach was proposed in [30] for energy management of the battery-Supercapacitor HESS for EV. The proposed controller was tested to consider the speed of two standard drive cycles and the slope of a city road drive cycle. In [31], a genetic algorithm multi-objective optimization was applied to reduce the HESS sizing and extend the drive range of the EV. A fuzzy control strategy was used to split the power between the front and rear HESS to achieve improved performance. The proposed configuration was tested in three standard drive cycles and was successful to increase the driving range and reduce the HESS total weight. The sizing and optimization of energy management for an electric bus with dual motors and a clutch vehicle was presented in [32]. A novel convex programming-based approach was developed to maximize the vehicle electric-drive efficiency. The results proved optimized energy efficiency concerning the size of the two motors, the size of the battery, and the power flow control achieved by the proposed method. A comparative study was done to compare the control response of a non-linear model predictive control (NMPC), rule-base control and linear model predictive control (LMPC) for the battery supercapacitor HESS in EVs [33]. A Toyota Rav4EV model was tested and showed improved response of NMPC compared to LMPC. Different control was applied in HESS for EV in [34]. A two-stage neural network was used to control the SOC of the supercapacitor. This control strategy was used to extend the supercapacitor life and guarantee continuous hybridization. This concept was tested for three standard drive cycles and underwent both a simulation and an experiment. The performance of a rule-based and a fuzzy adaptive controller was compared and the results showed improvements in battery life. A fuzzy logic controller was used to control the HESS for EVs [35]. The aim of the controller was to split the load power between the battery and supercapacitor, regulate the DC bus voltage and monitor the SOC of the supercapacitor. The results showed that the proposed controller improved battery life by supplying the load energy from battery at a steady state and from the supercapacitor during the transients. Another work looked into the efficiency of recovery braking energy for HESS in EV [5]. The efficiency of the DC-DC converters was studied under two different control strategies. The proposed HESS supplied fast load current to the system, resulting in increased EV performance and efficiency of regenerative energy. A real-time control strategy for HESS was studied in [36]. The optimization strategy was used to tackle three main problems, namely, power loss, load ripple and the stability of DC link voltage. The no-preference and weighted methods were used to handle the multi-objective problem in HESS. The HESS model and controller algorithm was tested using ADVISOR. The results showed smooth battery current flow and stable DC link voltage for both the simulation and experiment. Terrain information was explored to reduce fuel consumption of hybrid EVs in [37]. Fuel consumption improved depending on vehicle speed, control algorithm, road slope and battery size.

The above review reveals a research gap in terms of the effect of road slopes and traffic information on the design of the energy storage system in EVs. Ignoring road conditions can lead to incorrect estimation of the total energy demand in a drive cycle. An uphill drive consumes more energy when the vehicle accelerates, while less energy is used when the vehicle goes downhill. There are several methods used to measure a road's elevation and slope such as DEM, GPS and CPS [19], [38]. Vehicle-to-vehicle communications can also be used to collect information regarding a road's slope [39]. A Contour Positioning System (CPS) can be used to determine the contours, slope and angles of a road based on the road contour distance and elevation [38]. The information gathered using CPS can be used to estimate the quantity of energy needed to operate an EV to reach a particular destination. The CPS can be used to control the HESS of the EV on the road, instead of being used for monitoring purposes only.

This research looked into a semi-active HESS for use in EVs. The proposed control algorithm aimed to split the vehicle demand current between battery and supercapacitor optimally to extend battery life and ensure continuous HESS hybridization. The battery provides low traction current, while the supercapacitor supplies peak traction current and absorbs the regenerated current during braking. The CPS was used to determine the slope of the road for three different real drive cycles. The proposed control algorithm increased the number of possible repeated drive cycles for any real drive cycle compared with the online adaptive energy management system in the literature. The effect of the road slope the power demand was presented in this work. The energy management strategy contains three control layers to manage the power flow between the battery and supercapacitor. The first layer is an adaptive control that aims to obtain the optimal energy sharing percentage, R, between the battery and supercapacitor offline, before the vehicle moves for any selected drive cycle, depending on the road slope and vehicle speed. The second layer is a rule-based controller that aims to determine the optimal reference current for the supercapacitor during the journey online. The third layer is the LQR control to drive the bidirectional DC-DC converter by changing the duty cycle of the PWM online.

This research article is organized as follows: section II contains the system's modeling and configuration. Section III discusses the Contour Positioning System (CPS) and calculations for slopes in the road for an uphill, downhill and city tour drive cycle. Section IV discusses the design of the adaptive rule-based controller and the tuning methods. The simulation results and the controller's responses are explained

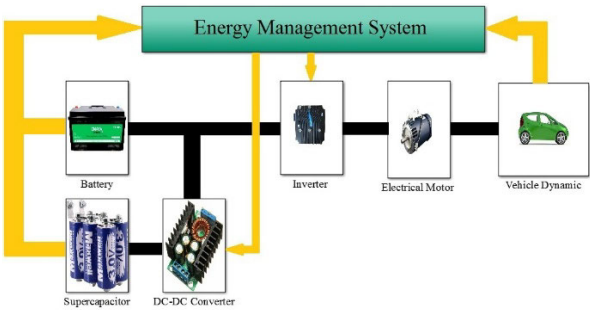


**FIGURE 2.** Architecture of HESS for Electric Vehicle in this research.

**TABLE 1.** The parameters of battery model.

| Parameter | Value |
|---|---|
| Capacity (Ah) | 100 |
| Internal Resistance (Ohms) | 0.125 |
| Nominal voltage (V) | 500 |
| Stored energy (kWh) | 50 |

in section V, while section VI provides a summary and concludes this research.

## II. SYSTEM MODELING AND CONFIGURATION

The semi-active HESS shown in Figure 1(b) was used in this work to deliver the required energy for the EV. The controller was designed to split the demand power between the battery and supercapacitor, and in turn limit battery current. The battery provides low traction and a steady state load current, while the supercapacitor supplies the peak demand current and absorbs the regenerative energy during braking. The adaptive rule-based controller was designed to manage the power flow from the supercapacitor by tuning the drive cycle of the DC-DC converter. Figure 2 shows the HESS architecture for the EV.

### A. BATTERY MODEL

The behavior of a battery has been heavily researched. Among the most popular models is the equivalent circuit model. This model is based on one of the following: runtime based model, impedance model, or thevenin model [40]–[42]. The non-linear dynamic model was investigated in terms of the battery's state-of-charge and electrolyte temperature [43]. Different research identified the parameter values for the equivalent circuit model by using the parameter estimation strategy [44]. The MATLAB/Simulink/-SimPowerSystems library shows the embedded model of the battery, and the relationship between its parameters as per Equation (1). Table 1 shows the main parameters of the battery model used in this study.

$$\begin{cases} V_b(t) = E_b(t) - r_b.i_b(t) \\ SOC(t) = 100\left(SOC(0) - \dfrac{1}{Q}\displaystyle\int_0^t i(t)\,dt\right) \end{cases} \quad (1)$$

**TABLE 2.** The parameters of supercapacitor model.

| Parameter | Value |
|---|---|
| Rated voltage (V) | 300 |
| Rated capacitance (F) | 100 |
| Resistance (mΩ) | 2.1 |

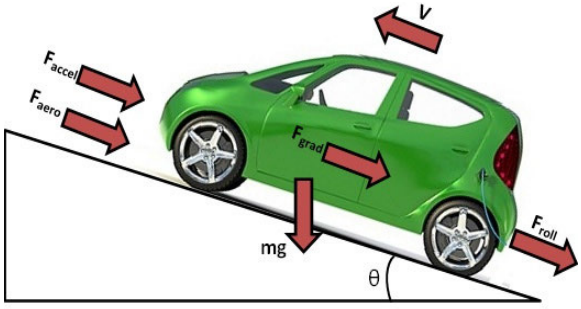


**FIGURE 3.** The Forces affect the vehicle during movement.

### B. SUPERCAPACITOR MODEL

In energy management systems, mathematical models of the energy storage devices must involve the dynamics of the energy storage device, and have high robustness. Many studies have surveyed supercapacitor models [45]. The model is usually composed of an equivalent electrical circuit, and the terminal measurements for charging and discharging the supercapacitor used to estimate the parameter of a supercapacitor model [46], [47]. MATLAB/Simulink/SimPowerSystems was used to model the supercapacitor in this research. Table 2 lists the parameters of the supercapacitor module used in this study. The terminal voltage $V_{sc}$ and the total capacity $C_{sc}$ of the supercapacitor module can be calculated as per Equation 2.

$$\begin{cases} C_{sc} = \dfrac{C_{cell}.N_{parallel}}{N_{series}} \\ V_{sc} = V_{cell}.N_{series} \end{cases} \quad (2)$$

### C. DC-DC CONVERTER MODEL

The state-space average model is among the techniques to model the DC-DC converter. This method is used to find the linearization of the non-linear behavior of the DC-DC converter [48], [49]. The system identification technique is another method used to identify the equivalent transfer function of the DC-DC converter [50]. The components of the DC-DC converter model can be identified using the MATLAB/Simulink/SimPowerSystems library [51]. To simplify the DC-DC converter model and decrease the simulation time, the switching elements (IGBT) in the DC-DC converter model can be replaced by current and voltage sources [52], [53]. The ON and OFF states matrices of the DC/DC converter can be derived using Equation 3. as shown at the bottom of the next pahe, While, $X = \begin{bmatrix} I_L & V_C \end{bmatrix}^T \equiv$ State Vector

**TABLE 3.** The parameters of electric vehicle model.

| *Parameter* | Value |
|---|---|
| Mv ≡ Vehicle Mass [kg] | 1325 |
| Cd ≡ Drag coefficient | 0.26 |
| Af ≡ Frontal area [$m^2$] | 2.57 |
| Wheel radius [m] | 0.3 |
| μrr ≡ rolling resistance | 0.0048 |
| g ≡ Gravity acceleration (g) [$ms^{-2}$] | 9.8 |
| ρ ≡ Air density [$kgm^{-3}$] | 1.29 |
| θ ≡ Road angle [radian] | Variable |
| V ≡ Vehicle Speed [ Km/h] | 50, 60, 70 |

### D. ELECTRIC VEHICLE MODEL

A proper model representing the EV's performance is required to estimate better energy consumption. Many researchers used MATLAB/Simulink to develop the model for EVs, while others used ADVISOR or other similar software to perform comprehensive performance analyses of a wide range of vehicles [54]–[59]. The dynamic system of the vehicle was explained clearly in [1], [60], [61]. In terms of the fundamentals of the vehicle dynamics, the total forces affecting the vehicle's momentum are aerodynamic force ($F_{aero}$), rolling force ($F_{roll}$), grading force ($F_{gr}$) and acceleration force ($F_{accel}$), as defined in Equation 4.

$$\sum F_{Total} = F_{aero} + F_{roll} + F_{grad} + F_{accel} \tag{4}$$

where:

$$\begin{aligned} F_{aero} &= 0.5.\rho.A_f.C_d.V^2 \\ F_{roll} &= \mu_{rr}.M_V.g.\cos\theta \\ F_{grad} &= M_V.g.\sin\theta \\ F_{accel} &= M_V.\frac{\partial V}{\partial t} \end{aligned}$$

MATLAB/Simulink/Vehicle Component library was used to model the behavior of the EV. Table 3 shows the main coefficients of the EV model. Figure 4 shows the completed model of the EV's HESS using MATLAB/Simulink. The inverter and the induction motor were used for the inner loop intelligent controller, as in [62], [63].

## III. CONTOUR POSITIONING SYSTEM

Road elevation is an important factor which affects energy consumption in EVs. Total energy consumption in EVs are affected by 15% to 20% when slopes in a road are taken into account [64]. There are many available data sources for deriving road information such as Google Maps, Intermap and Google Earth. Contour Positioning Systems (CPSs)

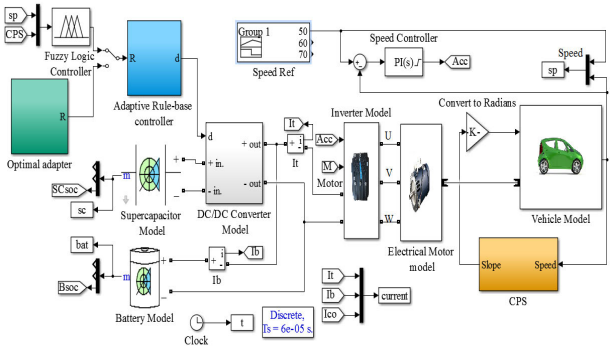


**FIGURE 4.** The HESS model for EV in MATLAB/Simulink.

use road information (i.e. elevation and distance) to calculate slopes in a road, as Equation 5.

$$\begin{cases} \angle\theta = \dfrac{|\Delta E|}{\Delta E} \times \sin^{-1}\dfrac{|\Delta E|}{\Delta D} \\ \Delta D\,(k) = D\,(k) - D(k-1) \\ \Delta E\,(k) = E\,(k) - E(k-1) \end{cases} \tag{5}$$

$$\text{While:} \begin{cases} D\,(k) = \text{Distance} \\ D\,(k-1) = \text{Previous Distance} \\ \Delta D = \text{Distance Difference} \\ E\,(k) = \text{Elevation} \\ E\,(k-1) = \text{Previous Elevation} \\ \Delta E = \text{ElevationDifference} \end{cases}$$

For this research, the driver needs to set the desired destination before starting the journey in the EV. The automated CPS obtains the road slope in terms of elevation, and uses this data to estimate the total energy consumption for the drive cycle. Google Earth was used as a source of topography information to obtain the road elevation. This study uses three real routes, namely, uphill, downhill and city tour, to investigate the influence of slopes of the road on the EV's energy consumption. Figure 5 shows the road's elevation profile against the distance for uphill, downhill and city tour used in this research. The CPS and the vehicle speed were used to control and estimate the required energy consumption for each drive cycle.

The uphill data was obtained for the drive from Berinchang (4°29'30.16''N 101°23'15.65''E) to Equatorial Hotel (4°30'17.64''N 101°24'31.18''E) in Cameron Highlands, Malaysia. The distance covered was five kilometers, and the elevation at the starting and destination points were 1496 m

$$\begin{cases} \dot{\bar{X}} = \begin{bmatrix} \dfrac{R.r_C\,(d-1) - r_L(R+r_C)}{L(R+r_C)} & \dfrac{R.(d-1)}{L(R+r_C)} \\ \dfrac{R.(1-d)}{C(R+r_C)} & -\dfrac{1}{C(R+r_C)} \end{bmatrix} X + \begin{bmatrix} \dfrac{1}{L} \\ 0 \end{bmatrix} V_{SC} \\ V_{CO} = \begin{bmatrix} \dfrac{R.(d-1)}{(R+r_C)} & \dfrac{R}{(R+r_C)} \end{bmatrix} X \end{cases} \tag{3}$$

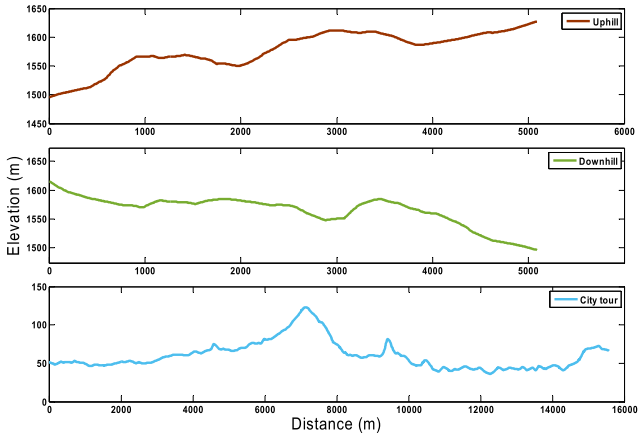


**FIGURE 5.** The road elevation for uphill, downhill and city tour.

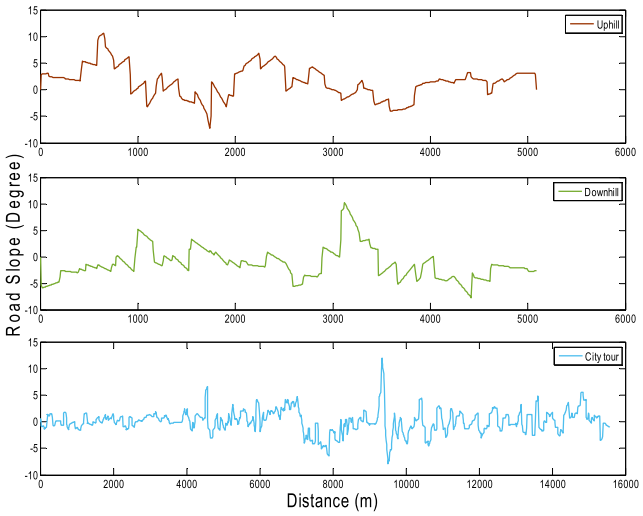


**FIGURE 6.** The road slope for uphill, downhill and city tour.

and 1627 m, respectively, which were measured every ten meters. CPS was used to obtain the data and calculate the road's slope along the journey. Meanwhile, the downhill elevation started from 1615 m, going down to 1496m. The total distance travelled was five kilometers, and the elevation was measured every ten meters. Meanwhile, the city tour involved traveling from University Tunku Abdul Rahman (UTAR) old campus in Setapak, Kuala Lumpur, to Technology Park Malaysia (TPM) in Bukit Jalil. Here, the elevation levels at the starting and destination points were 61 m and 66 m respectively. The total distance for the city tour was 15.85 kilometers, and the elevation was measured every ten meters. The elevation profile of the three journeys was used to measure the road slope, which was calculated by CPS using Equation 5. Figure 6 shows the road slope angles measured in degrees for the uphill, downhill and city tour.

## IV. CONTROL STRATAGEY

This study aims to extend the battery life-cycle for EVs by reducing operational stress for any type of drive cycle. An adaptive rule-based controller was used to distribute the total operational current of an EV between the HESS's battery and supercapacitor. The output current of the DC-DC converter $I_{co}(t)$ was controlled by the adaptive rule-based controller to manage the energy output of the supercapacitor. The total vehicle load current $I_t$ (t) is defined as per Equation 6.

$$I_t(t) = I_b(t) + I_{co}(t) \tag{6}$$

The adaptive rule-based controller allocated the HESS's current instantaneously for different drive cycles. The controller limited the battery current $I_b(t)$ to a desired value $I_{b\_max}$, and split the current between the battery and supercapacitor during any drive cycle. The road's slope and the vehicle speed are important factors that affect an EV's energy consumption. The controller was designed to manage the HESS's energy flow under various conditions, accounting for total demand load current $I_t(t)$, supercapacitor state of charge $SC_{soc}$ and the direction of the energy flow. The controller's working conditions were defined as per Equation 7. as shown at the bottom of the next page, The rule-based controller allows the HESS to supply the EV with current from the battery when the total load current of the EV is less than the maximum value of battery current $I_{b\_max}$. The controller also limits the battery current to $I_{b\_max}$ during a high load drive cycle. On the other hand, the supercapacitor absorbs all the regenerative energy during the drive cycle. The total regenerative energy that could be absorbed by the supercapacitor from the initial voltage to the final voltage is defined as per Equation 8. The state of the charge condition for the supercapacitor is defined as per Equation 9.

$$\Delta En_{SC} = \frac{C_0}{2}(V_{sc}(0) - V_{sc}(t)) \tag{8}$$

$$SOC_{sc\_max} \geq SOC_{sc} > SOC_{sc\_min} \tag{9}$$

As mentioned above, the EV's destination was selected before the journey initiated. The adaptive algorithm estimates the total current demand needed for the drive cycle and the regenerative current depending on the road's slope, vehicle speed and the parameters of the EV model. The percentage power split between the battery and supercapacitor (R) in HESS can be determined in several independent ways. Two methods were investigated to adapt the rule-based controller in terms of energy split between battery and supercapacitor. The first is the optimal method that compares the total current demand and regenerative current of the electric vehicle during the drive cycle. The second is a fuzzy adaptive rule-based controller using a fuzzy logic controller. The sharing percentage (R) was used to regulate the controller to save energy during the drive cycle. The adaptive rule-based controller is defined as per Equation 10. as shown at the bottom of the next page.

### A. OPTIMAL ADAPTIVE RULE-BASE CONTROLLER

In this method, the percentage of current shared between the battery and supercapacitor in HESS is tuned on time for the distance of the specific drive cycle. After setting the destination and the road's slope calculated by CPS,

the system estimates the total energy required for the drive cycle. The road slope and the vehicle's approximated speed are considered along the journey to the desired destination. The accumulation method for the positive supplied current $I_{tp}$ and the regenerative current $I_{reg}$ during the drive cycle was applied. The split percentage was set by comparing the total current demand and regenerative current of the EV during the drive cycle. The positive supplied current $I_{tp}$ and the regenerative current $I_{reg}$ are defined as per Equation 11.

$$\begin{cases} I_{reg} = \sum_{0}^{t} I_t(t) & I_t < 0 \\ I_{tp} = \sum_{0}^{t} I_t(t) & I_t > 0 \end{cases} \tag{11}$$

This method reduces battery stress and saves energy inside the HESS. The system predicts the approximate amount of the regenerative energy, depending on the road's slope. Then, the percentage of power split between the battery and the supercapacitor (R) is set to ensure that the HESS is working properly and the supercapacitor is able to absorb all the regenerative energy during the drive cycle. Figure 7 presents the flowchart of optimal adaptive rule-base controller.

### B. FUZZY ADAPTIVE RULE-BASE CONTROLLER

Most research in the literature on road terrain information takes the instant effect of the road slope in the control action. In this method, the value of current shared between the battery and supercapacitor in HESS varies during the drive cycle. A fuzzy logic controller was used to manipulate the percentage of current shared between the battery and supercapacitor during the journey. The road's slope and vehicle speed are inputs for the fuzzy logic controller in controlling the journey. Figure 8 shows the surface plot of the fuzzy logic controller which represents the relationship between the inputs (road slope and vehicle speed) and the percentage of power shared between the battery and supercapacitor, R. Here, the supercapacitors assist the battery to deliver the load current continuously with different percentages along the drive cycle. Furthermore, the operation effect of this controller is shown in Figure 9.

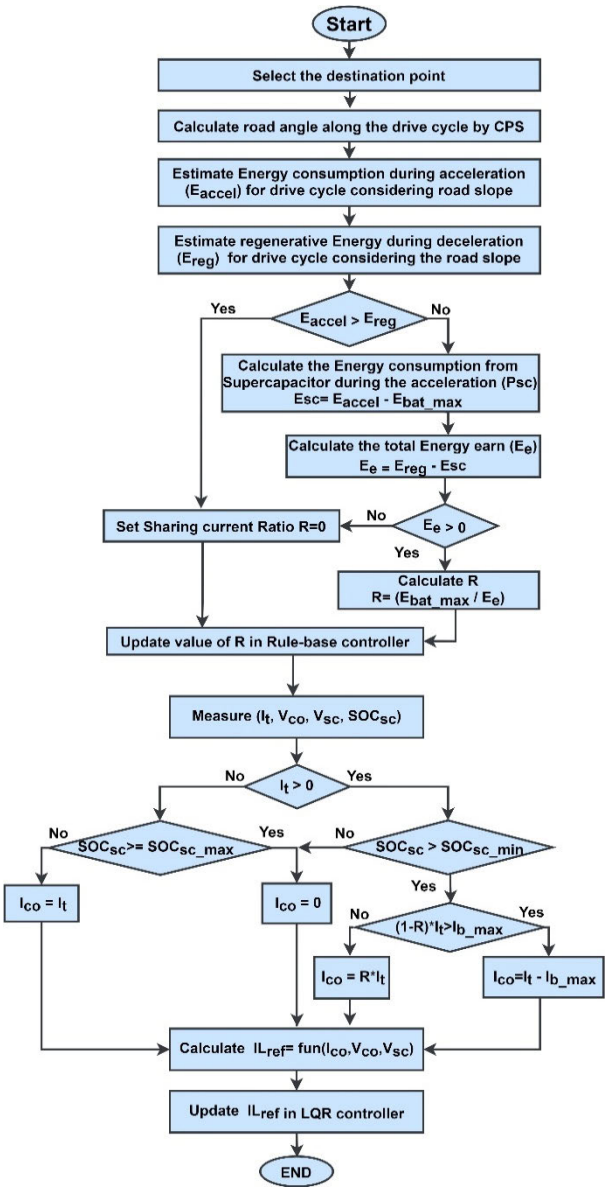


**FIGURE 7.** Flowchart of optimal adaptive rule-base controller.

### C. LINEAR QUADRATIC REGULATOR (LQR)

LQR is a control method that depends on generated feedback gains to improve the system response by controlling one state of the model. Equation 12 represents the cost function for a

$$\begin{cases} \textbf{If } (I_t > 0) \textbf{ and } (I_t < I_{b\_max}) \textbf{ then} & I_{co} = 0 \\ \textbf{If } (I_t > 0) \textbf{and } \left(I_t > I_{b\_max}\right) \textbf{ and } (SOC_{sc} > SOC_{sc\_min}) \textbf{ then} & I_{co} = (I_t - I_{b\_max}) \\ \textbf{If } (I_t < 0) \textbf{ and } (SOC_{sc} < SOC_{sc\_max}) \textbf{ then} & I_{co} = I_t \end{cases} \tag{7}$$

$$\begin{cases} \textbf{If } (I_t > 0) \textbf{and } \left((1-R)\, I_t < I_{b_{max}}\right) \textbf{ and } (SOC_{sc} > SOC_{sc\_min}) \textbf{ then} & I_{co} = I_t * R \\ \textbf{If } (I_t > 0) \textbf{and } \left((1-R)\, I_t > I_{b_{max}}\right) \textbf{ and } (SOC_{sc} > SOC_{sc_{min}}) \textbf{ then} & I_{co} = (I_t - I_{b\_max}) \\ \textbf{If } (I_t < 0) \textbf{and } (SOC_{sc} < SOC_{sc\_max}) \textbf{ then} & I_{co} = I_t \end{cases} \tag{10}$$

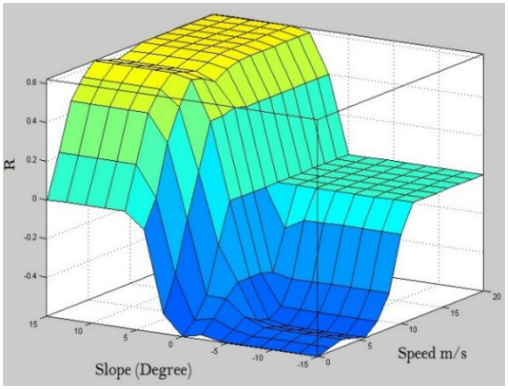


**FIGURE 8.** The fuzzy logic controller surface.

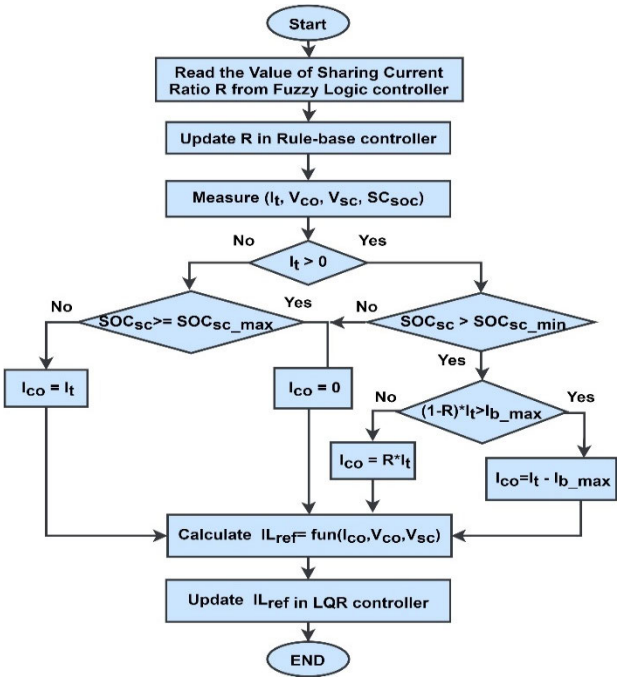


**FIGURE 9.** Flowchart of Fuzzy adaptive rule-base controller.

continuous-time linear.

$$J(u) = \int_0^\infty \left(x^T Qx + u^T Ru + 2x^T Nu\right) dt \tag{12}$$

In this research, the objective of LQR is to drive the DC-DC converter to supply the desired current from the supercapacitor module. The output power of the DC-DC converter is controlled by varying the duty cycle of the Pulse Width Modulation (PWM). LQR was selected due to its simplicity and easy implementation, and the feedback gains can be directly obtained from the matrices of the DC-DC converter model. Moreover, the close-loop response of LQR is stable and is insensitive to external disturbances [65]. The modeling of the DC-DC converter considered switching states of the IGBT as follows:

$$\dot{x} = [dA_{ON} + (1-d)A_{OFF}]X + [dB_{ON} + (1-d)B_{OFF}]V_{sc} \tag{13}$$

where:

$$\begin{cases} d = The\ switching\ period \\ A_{on.off} = State\ matrices \\ B_{on.off} = Control\ matrices \end{cases}$$

The following matrices represent the state and control matrices of the DC-DC converter in ON and OFF states:

$$X = \begin{bmatrix} I_L & V_c \end{bmatrix}^T = state\ vector$$

$$A_{ON} = \begin{bmatrix} -\frac{r_L}{L} & 0 \\ 0 & \frac{-1}{C.(R+r_C)} \end{bmatrix}, B_{ON} = \begin{bmatrix} \frac{1}{L} \\ 0 \end{bmatrix},$$

$$A_{OFF} = \begin{bmatrix} \frac{-R.r_C - R.r_L - r_C.r_L}{L(R+r_C)} & -\frac{R}{L(R+r_C)} \\ \frac{R}{C(R_o+R_c)} & -\frac{1}{C(R_o+R_c)} \end{bmatrix},$$

$$B_{OFF} = \begin{bmatrix} \frac{1}{L} \\ 0 \end{bmatrix}$$

The state-space model of the DC/DC converter is represented by the following equations [66]:

$$\frac{d}{dt}\begin{bmatrix} i_L \\ V_c \end{bmatrix} = \begin{bmatrix} \frac{R.r_C.(d-1) - r_L(R+r_C)}{L(R+r_C)} & \frac{R.(d-1)}{L(R+r_C)} \\ \frac{R.(1-d)}{C(R+r_C)} & -\frac{1}{C(R+r_C)} \end{bmatrix} \times \begin{bmatrix} i_L \\ V_c \end{bmatrix} + \begin{bmatrix} \frac{1}{L} \\ 0 \end{bmatrix} V_{sc} \tag{14}$$

$$V_{co} = \begin{bmatrix} \frac{R.(d-1)}{(R+r_C)} & \frac{R}{(R+r_C)} \end{bmatrix} \begin{bmatrix} i_L \\ v_c \end{bmatrix} \tag{15}$$

$$\begin{cases} A_s = A = dA_{ON} + (1-d)A_{OFF} \\ B_d = (A_{ON} - A_{OFF})X - (B_{ON} - B_{OFF})V_{sc} \\ B_s = \begin{bmatrix} B_d & B \end{bmatrix} \end{cases} \tag{16}$$

$$B_d = \begin{bmatrix} \frac{R.r_C}{L(R+r_C)}.i_L + \frac{R.r_C}{L(R+r_C)}.V_c \\ -\frac{R}{C.(R+r_C)}.i_L \end{bmatrix} \tag{17}$$

## V. RESULTS AND DISCUSSION

This research work designed an HESS to manage and control the energy flow in EVs. Figure 4 shows the model that integrates the HESS model, controllers and the EV model considering CPS. The system was modeled using MATLAB/Simulink to investigate the HESS's response and performance of an adaptive rule-based controller involving three real-life journeys with various road slopes and three different speeds. First, the effect of a road's slope in pure battery EV was investigated. The comparison was presented between the battery state of charge considering a road's slope (measured using CPS) against the battery state of charge ignoring the slope for the same working condition, and drive cycle in a

**TABLE 4.** The effect of including road slope for battery SOC in EV.

| *Speed* | | $SOC_b(0)$ | $SOC_b(t)_{slope=0}$ | $SOC_b(t)_{slope=CPS}$ | $EnVar$ |
|---|---|---|---|---|---|
| 50 Km/h | Uphill | 0.95 | 0.9407 | 0.9321 | 0.91% |
| | Downhill | 0.95 | 0.9407 | 0.9482 | -0.79% |
| | City Tour | 0.95 | 0.9231 | 0.9216 | 0.16% |
| 60 Km/h | Uphill | 0.95 | 0.9385 | 0.9303 | 0.86% |
| | Downhill | 0.95 | 0.9385 | 0.9458 | -0.77% |
| | City Tour | 0.95 | 0.9165 | 0.9151 | 0.15% |
| 70 Km/h | Uphill | 0.95 | 0.9360 | 0.9278 | 0.86% |
| | Downhill | 0.95 | 0.9360 | 0.9432 | -0.77% |
| | City Tour | 0.95 | 0.9095 | 0.9090 | 0.05% |

pure battery EV. Table 4 shows the initial values of the state of charge for battery $SOC_b$ (0), final values of state of charge for battery ignoring a road's slope $SOC_b$ $(t)_{slope=0}$, final values of state of charge for battery considering the road's slope CPS $SOC_b$ $(t)_{slope=CPS}$ and the Energy Variance ($EnVar$) for three different drive cycles and speeds. The results demonstrate that the EV (using CPS) consumed more energy going uphill, taking up to 0.9% of the total energy. On the other hand, the EV (using CPS) earned energy going downhill, taking up to 0.79% of the total energy. Meanwhile, a small difference in energy consumption was recorded for the city tour (using CPS). The energy variance was calculated as per Equation 18. as shown at the bottom of the page, In order to investigate, analyze and validate the proposed design of the optimal adaptive rule-based controller and the fuzzy adaptive rule-based controller for HESS, simulations were run for uphill, downhill and city tour drive cycles, at three different speeds (50Km/h, 60Km/h and 70 Km/h). The results of uphill, downhill and city tour with a speed of 50Km/h were presented and explained in details, while the results of speeds 60Km/h and 70 Km/h were summarized in the tables. The state of charge for the HESS's battery and supercapacitor were compared for both controllers for different journeys, to validate their performance and the energy savings in each scenario. The value of initial state of charge for the battery $SOC_b$ (0) and supercapacitor $SOC_{SC}$ (0) was 0.95 and 0.9224 respectively. The final value of state of charge for the battery $SOC_b$ $(t)_{CPS}$ and supercapacitor $SOC_{SC}$ $(t)_{CPS}$ were measured at the end of the journeys and the percentage of energy consumption for both was given by Equation 19. as shown at the bottom of the page, In the uphill drive cycle, the EV consumed more energy to maintain its acceleration. Here, the optimal algorithm adapts the rule-base controller before the vehicle starts moving, considering the desired destination and CPS.

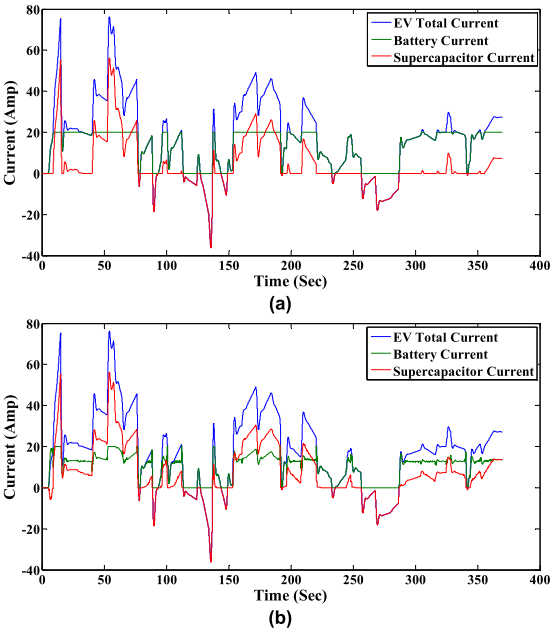


**FIGURE 10.** HESS current for EV based on 50Km/h Uphill journey. (a) Optimal adaptive. (b) Fuzzy adaptive.

The fuzzy adaptive rule-based calculated the HESS's percentage share of current between the battery and supercapacitor instantaneously during the drive. Figure 10 shows the HESS's current allocation in the EV during the uphill journey for both controllers. The battery current was smooth and limited by $I_{b\_max}$, while the regenerative current was absorbed by the supercapacitor.

In the 50Km/h Uphill drive cycle, the optimal adaptive rule-based controller for HESS consumed 1.43% of the total stored energy of the battery, and 11.35% of the total energy of the supercapacitor. Meanwhile, the fuzzy adaptive rule-based controller for HESS consumed 1.09% of the total stored energy of the battery, and 20.70% of the total energy of the supercapacitor, for the same journey and conditions. Figure 11(a) represents the battery SOC for both controllers, and the battery SOC in pure battery EV for equivalent drive cycle and speed. Figure 11(b) illustrates the changes in supercapacitor SOC during the uphill drive cycle.

For the 50Km/h downhill drive cycle, the EV can regenerate energy when the vehicle brakes. The adaptive rule-based controller stores the energy in the supercapacitor. Figure 12

$$\text{EnVar} = \frac{\left(\text{SOC}_\text{b}\,(0) - \text{SOC}_\text{b}\,(\text{t})_{\text{slope=CPS}}\right) - \left(\text{SOC}_\text{b}\,(0) - \text{SOC}_\text{b}\,(\text{t})_{\text{slope=0}}\right)}{\text{SOC}_\text{b}(0)} \times 100 \tag{18}$$

$$\begin{cases} \text{Battery Consumption} = \dfrac{\text{SOC}_\text{b}\,(0) - \text{SOC}_\text{b}\,(\text{t})_{\text{CPS}}}{\text{SOC}_\text{b}\,(0)} \times 100 \\ \text{Supercapacitor Consumption} = \dfrac{\text{SOC}_{\text{SC}}\,(0) - \text{SOC}_{\text{SC}}\,(\text{t})_{\text{CPS}}}{\text{SOC}_{\text{SC}}\,(0)} \times 100 \end{cases} \tag{19}$$

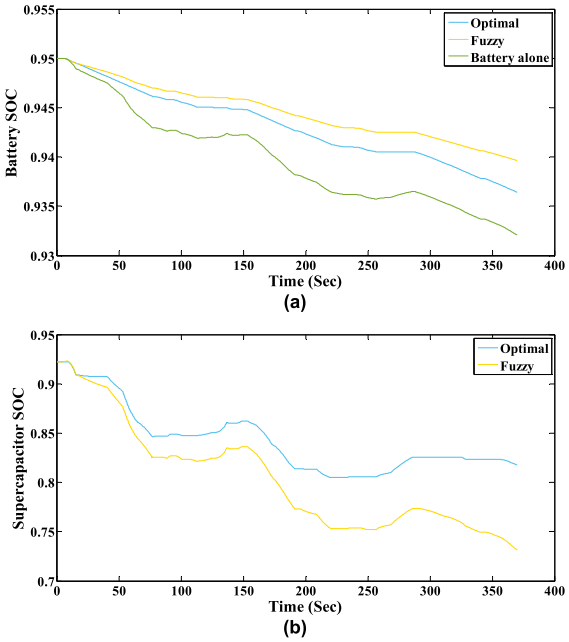


**FIGURE 11.** HESS SOC based on 50Km/h Uphill journey (a)Battery. (b) Supercapacitor.

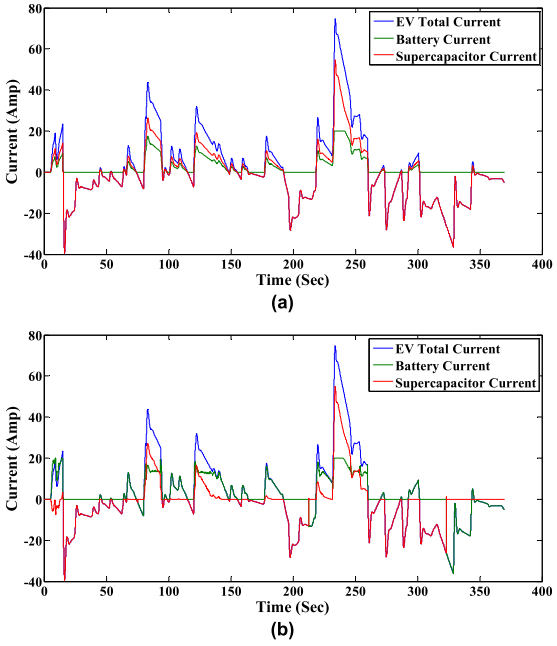


**FIGURE 12.** HESS current for EV based on 50Km/h Downhill journey (a) Optimal adaptive. (b) Fuzzy adaptive.

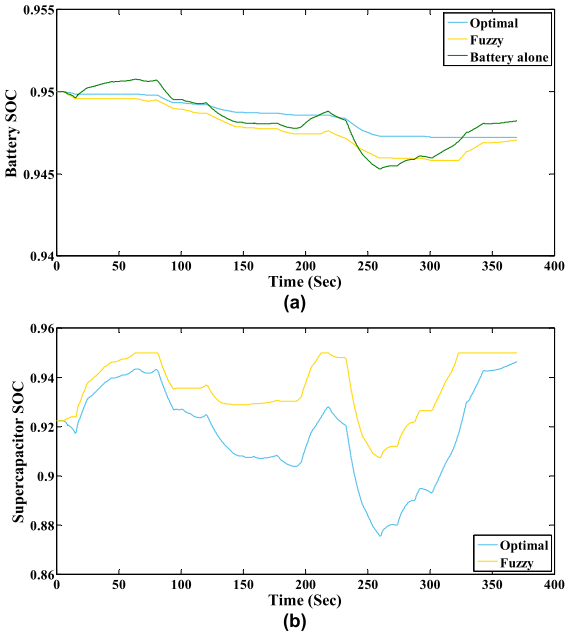


**FIGURE 13.** HESS SOC based on 50Km/h Downhill journey (a)Battery. (b) Supercapacitor.

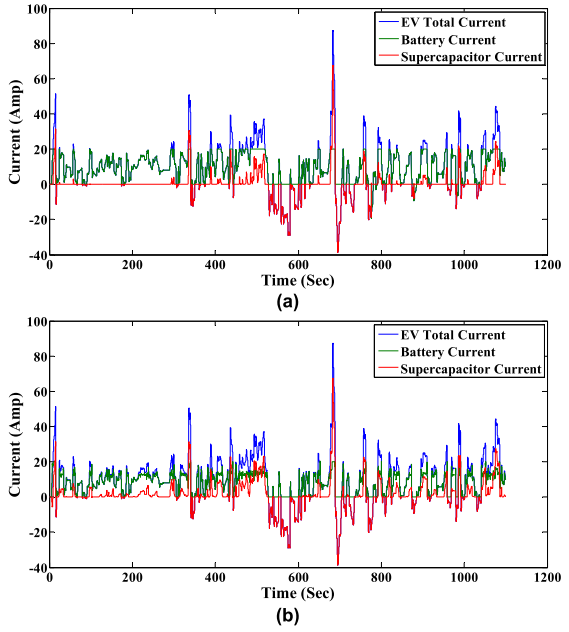


**FIGURE 14.** HESS current for EV based on 50Km/h City tour journey (a) Optimal adaptive. (b) Fuzzy adaptive.

shows the HESS's current consumption in the EV based on the downhill journey for both controllers.

In the 50Km/h downhill drive cycle, the optimal adaptive rule-based controller for HESS consumed 0.3% of the total stored energy of the battery, and gained 2.6% of the total energy for the supercapacitor.

Meanwhile, the fuzzy adaptive rule-based controller for HESS consumed 0.31% of the total stored energy of the battery, and gained 3% of the total energy for the supercapacitor, for the same journey and conditions. Figure 13 shows the changes in battery and supercapacitor SOC during the downhill drive cycle.

For 50Km/h city tour drive cycle, the HESS's performance (using CPS) did not witness any major effect. Figure 14 shows the HESS's current consumption in the EV during the city tour for both controllers.

The optimal adaptive rule-based controller for HESS consumed 3.03% of the total stored energy of the battery, and gained 0.95% of the total energy of the supercapacitor.

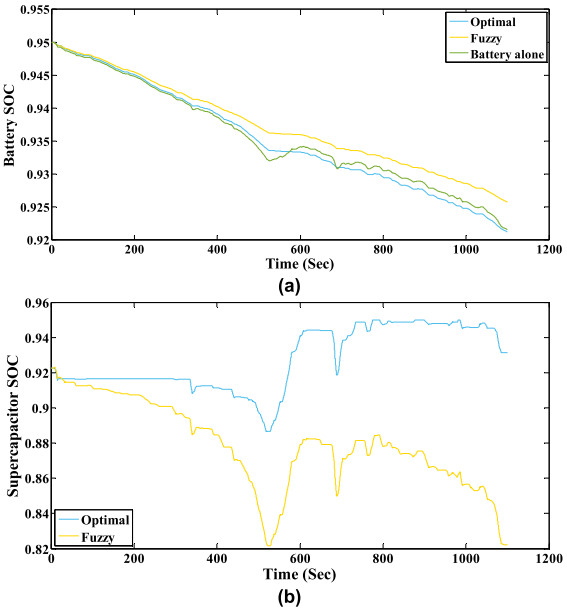


**FIGURE 15.** HESS SOC based on 50Km/h Downhill journey (a)Battery. (b) Supercapacitor.

Meanwhile, the fuzzy adaptive rule-based controller for HESS consumed 2.55% of the total stored energy of the battery, and 10.89% of the total energy of the supercapacitor, for the identical conditions. Figure 15 shows the changes in battery and supercapacitor SOC during the city tour drive cycle.

Table 5 presents the values of final state of charge for the battery and supercapacitors of HESS by using optimal and fuzzy adaptive controllers in the various drive cycles at a speed of 50Km/h. The total percentage of energy consumption for the battery and supercapacitor and the number of possible repeated drive cycles in every case were presented. The results of the energy consumption for HESS show that both controllers were successful to reduce the battery stress during EV acceleration and deceleration, as compared to using a pure battery electric vehicle.

Furthermore, the results of optimal adaptive controller show that it manages the energy of supercapacitor better than the fuzzy adaptive controller in terms of continuous hybridization for a higher number of drive cycles. In addition, Tables 6 and 7 present the results of the optimal adaptive r and the fuzzy adaptive controllers for HESS for 60 Km/h and 70 Km/h respectively. The results demonstrate that the proposed optimal adaptive controller effectively enhanced the performance of the HESS for the EV in a wide range of cycles and speeds.

The current limitation of the proposed design is that it requires the driver to define the destination and the driving speed before the vehicle starts. However, there is difficulty in determining the appropriate vehicle speed for the selected journey by the driver. Furthermore, changing the destination path or the vehicle speed during the journey leads to change in the total energy consumption of the drive cycle, which requires a new calculation for the energy sharing percentage R between the battery and supercapacitor.

In future work, an algorithm to automatically estimate the proper speed of the selected journey will be proposed. On the other hand, in case of changing the destination or the vehicle speed during the journey, the Adaptive algorithm will be improved to update the value of the sharing percentage R for the controller. In addition, to validate whether the proposed method is suitable to perform practically, experimental work for HESS and electric vehicle emulators will be implemented.

**TABLE 5.** The SOC of Battery and supercapacitor in speed 50 Km/h.

| 50 Km/h | | Uphill | Downhill | City tour |
|---|---|---|---|---|
| Optimal adaptive controller | $SOC_b(t)_{CPS}$ | 0.9364 | 0.9472 | 0.9212 |
| | $SOC_{sc}(t)_{CPS}$ | 0.8177 | 0.9464 | 0.9312 |
| | Battery Consumption | 1.43% | 0.3% | 3.03% |
| | Supercapacitor Consumption | 11.35% | -2.6% | -0.95% |
| | No. Cycles | 6.6 | 250 | 24.8 |
| Fuzzy adaptive controller | $SOC_b(t)_{CPS}$ | 0.9396 | 0.9471 | 0.9258 |
| | $SOC_{sc}(t)_{CPS}$ | 0.7315 | 0.95 | 0.8220 |
| | Battery Consumption | 1.09% | 0.31% | 2.55% |
| | Supercapacitor Consumption | 20.70% | -3% | 10.89% |
| | No. Cycles | 3.6 | 242 | 6.9 |

**TABLE 6.** The SOC of Battery and supercapacitor in speed 60 Km/h.

| 60 Km/h | | Uphill | Downhill | City tour |
|---|---|---|---|---|
| Optimal adaptive controller | $SOC_b(t)_{CPS}$ | 0.9379 | 0.9451 | 0.9193 |
| | $SOC_{sc}(t)_{CPS}$ | 0.7309 | 0.9386 | 0.8211 |
| | Battery Consumption | 1.27% | 0.52% | 3.23% |
| | Supercapacitor Consumption | 20.76% | -1.47% | 10.98% |
| | No. Cycles | 3.6 | 144 | 6.8 |
| Fuzzy adaptive controller | $SOC_b(t)_{CPS}$ | 0.9390 | 0.9448 | 0.9215 |
| | $SOC_{sc}(t)_{CPS}$ | 0.7005 | 0.9461 | 0.7650 |
| | Battery Consumption | 1.16% | 0.55% | 3% |
| | Supercapacitor Consumption | 24.06% | -2.57% | 17.06% |
| | No. Cycles | 3.1 | 136 | 4.4 |

**TABLE 7.** The SOC of Battery and supercapacitor in speed 70 Km/h.

| 70 Km/h | | Uphill | Downhill | City tour |
|---|---|---|---|---|
| Optimal adaptive controller | $SOC_b(t)_{CPS}$ | 0.9390 | 0.9441 | 0.9191 |
| | $SOC_{sc}(t)_{CPS}$ | 0.6246 | 0.9028 | 0.6573 |
| | Battery Consumption | 1.16% | 0.62% | 3.25% |
| | Supercapacitor Consumption | 32.29% | 2.13% | 28.74% |
| | No. Cycles | 2.3 | 35 | 2.6 |
| Fuzzy adaptive controller | $SOC_b(t)_{CPS}$ | 0.9391 | 0.9441 | 0.9193 |
| | $SOC_{sc}(t)_{CPS}$ | 0.6209 | 0.9030 | 0.6531 |
| | Battery Consumption | 1.15% | 0.62% | 3.23% |
| | Supercapacitor Consumption | 32.69% | 2.1% | 29.2% |
| | No. Cycles | 2.3 | 35 | 2.6 |

## VI. CONCLUSION

Total energy consumption of an EV affected by topographical conditions was tested in three real drive cycles with different characteristics and speeds. The results of the simulations proved that an uphill drive consumed more energy, while regenerative energy increased going downhill. Meanwhile, it was found that a road's slope has a limited effect for a city tour drive cycle. The CPS was used to measure the road's slope along the drive cycles. The proposed HESS optimal adaptive rule-based and fuzzy adaptive rule-based controllers were successful in extending the battery life-cycle by limiting battery current during high load operations. Furthermore, the final state of charge for battery and supercapacitor were compared for three different drive cycles and speeds. The optimal adaptive rule-based controller performed better than the fuzzy adaptive rule-based controller in terms of continuous hybridization during more drive cycles.

## REFERENCES

[1] E. Schaltz, *Electrical Vehicle Design and Modeling*. London, U.K.: INTECH Open Access, 2011.

[2] J. Jordán, J. Palanca, E. del Val, V. Julian, and V. Botti, "A multi-agent system for the dynamic emplacement of electric vehicle charging stations," *Appl. Sci.*, vol. 8, p. 313, Dec. 2018.

[3] G. Ren, "Review of energy storage technologies for extended range electric vehicle," *J. Appl. Sci. Eng.*, vol. 22, pp. 69–82, May 2019.

[4] V. Paladini, T. Donateo, A. de Risi, and D. Laforgia, "Super-capacitors fuel-cell hybrid electric vehicle optimization and control strategy development," *Energy Convers. Manage.*, vol. 48, no. 11, pp. 3001–3008, Nov. 2007.

[5] Y. Li, X. Huang, D. Liu, M. Wang, and J. Xu, "Hybrid energy storage system and energy distribution strategy for four-wheel independent-drive electric vehicles," *J. Cleaner Prod.*, vol. 220, pp. 756–770, May 2019.

[6] O. Veneri, C. Capasso, and S. Patalano, "Experimental investigation into the effectiveness of a super-capacitor based hybrid energy storage system for urban commercial vehicles," *Appl. Energy*, vol. 227, pp. 312–323, Oct. 2018.

[7] C. Capasso, D. Lauria, and O. Veneri, "Experimental evaluation of model-based control strategies of sodium-nickel chloride battery plus supercapacitor hybrid storage systems for urban electric vehicles," *Appl. Energy*, vol. 228, pp. 2478–2489, Oct. 2018.

[8] P. Mellor, N. Schofield, and D. Howe, "Flywheel and supercapacitor peak power buffer technologies," in *Proc. Electr., Hybrid Fuel Cell Vehicles*, 2000, pp. 8-1–8-5.

[9] Y. Zhang, Z. Jiang, and X. Yu, "Control strategies for battery/supercapacitor hybrid energy storage systems," in *Proc. Energy Conf.*, 2008, pp. 1–6.

[10] F. Ju, Q. Zhang, W. Deng, and J. Li, "Review of structures and control of battery-supercapacitor hybrid energy storage system for electric vehicles," in *Proc. IEEE Int. Conf. Autom. Sci. Eng. (CASE)*, Taipei, Taiwan, Aug. 2014, pp. 143–148.

[11] S. F. Tie and C. W. Tan, "A review of energy sources and energy management system in electric vehicles," *Renew. Sustain. Energy Rev.*, vol. 20, pp. 82–102, Apr. 2013.

[12] J. Cao and A. Emadi, "A new Battery/UltraCapacitor hybrid energy storage system for electric, hybrid, and plug-in hybrid electric vehicles," *IEEE Trans. Power Electron.*, vol. 27, no. 1, pp. 122–132, Jan. 2012.

[13] C. Xiang, Y. Wang, S. Hu, and W. Wang, "A new topology and control strategy for a hybrid battery-ultracapacitor energy storage system," *Energies*, vol. 7, no. 5, pp. 2874–2896, Apr. 2014.

[14] A. Ostadi, M. Kazerani, and S.-K. Chen, "Hybrid energy storage system (HESS) in vehicular applications: A review on interfacing battery and ultracapacitor units," in *Proc. IEEE Transp. Electrific. Conf. Expo (ITEC)*, Jun. 2013, pp. 1–7.

[15] B. Long, S. Lim, Z. Bai, J. Ryu, and K. Chong, "Energy management and control of electric vehicles, using hybrid power source in regenerative braking operation," *Energies*, vol. 7, no. 7, pp. 4300–4315, Jul. 2014.

[16] Z. Song, J. Li, X. Han, L. Xu, L. Lu, M. Ouyang, and H. Hofmann, "Multi-objective optimization of a semi-active battery/supercapacitor energy storage system for electric vehicles," *Appl. Energy*, vol. 135, pp. 212–224, Dec. 2014.

[17] A. Wangsupphaphol, N. R. Nik Idris, A. Jusoh, N. D. Muhamad, and S. Chamchuen, "Acceleration-based control strategy and design for hybrid electric vehicle auxiliary energy source," *ECTI Trans. Comput. Inf. Technol.*, vol. 9, no. 1, pp. 83–92, Jan. 1970.

[18] M. Michalczuk, B. Ufnalski, and L. M. Grzesiak, "Fuzzy logic based power management strategy using topographic data for an electric vehicle with a battery-ultracapacitor energy storage," *Int. J. Comput. Math. Electr. Electron. Eng.*, vol. 34, no. 1, pp. 173–188, Jan. 2015.

[19] W. Han, Y. Li, and L. Chen, "High-precision DEM production in complex urban area using LiDAR data," in *Proc. 20th Int. Conf. Geoinformatics*, Jun. 2012, pp. 1–5.

[20] Q. Zhang and W. Deng, "An adaptive energy management system for electric vehicles based on driving cycle identification and wavelet transform," *Energies*, vol. 9, no. 5, p. 341, May 2016.

[21] J. Shen and A. Khaligh, "Design and real-time controller implementation for a battery-ultracapacitor hybrid energy storage system," *IEEE Trans. Ind. Informat.*, vol. 12, no. 5, pp. 1910–1918, Oct. 2016.

[22] K. V. S. Bharath and K. Pandey, "Fuzzy-based multi-objective optimization for subjection and diagnosis of hybrid energy storage system of an electric vehicle," in *Proc. Int. Conf. Intell. Commun., Control Devices*, 2017, pp. 299–307.

[23] A. Castaings, A. Bouscayrol, R. Trigui, and W. Lhomme, "Practical control schemes of a battery/supercapacitor system for electric vehicle," *IET Electr. Syst. Transp.*, vol. 6, no. 1, pp. 20–26, Mar. 2016.

[24] J. Shen and A. Khaligh, "Predictive control of a battery/ultracapacitor hybrid energy storage system in electric vehicles," in *Proc. IEEE Transp. Electrific. Conf. Expo (ITEC)*, Jun. 2016, pp. 1–6.

[25] O. Gomozov, J. P. F. Trovao, X. Kestelyn, and M. R. Dubois, "Adaptive energy management system based on a real-time model predictive control with nonuniform sampling time for multiple energy storage electric vehicle," *IEEE Trans. Veh. Technol.*, vol. 66, no. 7, pp. 5520–5530, Jul. 2017.

[26] L. Sun, K. Feng, C. Chapman, and N. Zhang, "An adaptive power-split strategy for battery–supercapacitor powertrain–design, simulation, and experiment," *IEEE Trans. Power Electron.*, vol. 32, no. 12, pp. 9364–9375, Dec. 2017.

[27] J. Hu, D. Liu, C. Du, F. Yan, and C. Lv, "Intelligent energy management strategy of hybrid energy storage system for electric vehicle based on driving pattern recognition," *Energy*, vol. 198, May 2020, Art. no. 117298.

[28] B. Zhao, C. Lv, and T. Hofman, "Driving-cycle-aware energy management of hybrid electric vehicles using a three-dimensional Markov chain model," *Automot. Innov.*, vol. 2, no. 2, pp. 146–156, Jun. 2019.

[29] S. Liu, X. Xie, and L. Yang, "Analysis, modeling and implementation of a switching bi-directional buck-boost converter based on electric vehicle hybrid energy storage for V2G system," *IEEE Access*, vol. 8, pp. 65868–65879, 2020.

[30] L. Zhang, X. Ye, X. Xia, and F. Barzegar, "A real-time energy management and speed controller for an electric vehicle powered by a hybrid energy storage system," *IEEE Trans. Ind. Informat.*, vol. 16, no. 10, pp. 6272–6280, Oct. 2020.

[31] J. J. Eckert, L. C. D. A. Silva, F. G. Dedini, and F. C. Correa, "Electric vehicle powertrain and fuzzy control multi-objective optimization, considering dual hybrid energy storage systems," *IEEE Trans. Veh. Technol.*, vol. 69, no. 4, pp. 3773–3782, Apr. 2020.

[32] X. Hu, Y. Li, C. Lv, and Y. Liu, "Optimal energy management and sizing of a dual motor-driven electric powertrain," *IEEE Trans. Power Electron.*, vol. 34, no. 8, pp. 7489–7501, Aug. 2019.

[33] P. Golchoubian and N. L. Azad, "Real-time nonlinear model predictive control of a battery–supercapacitor hybrid energy storage system in electric vehicles," *IEEE Trans. Veh. Technol.*, vol. 66, no. 11, pp. 9678–9688, Nov. 2017.

[34] K. Alobeidli and V. Khadkikar, "A new ultracapacitor state of charge control concept to enhance battery lifespan of dual storage electric vehicles," *IEEE Trans. Veh. Technol.*, vol. 67, no. 11, pp. 10470–10481, Nov. 2018.

[35] M. Sellali, S. Abdeddaim, A. Betka, A. Djerdir, S. Drid, and M. Tiar, "Fuzzy-super twisting control implementation of battery/super capacitor for electric vehicles," *ISA Trans.*, vol. 95, pp. 243–253, Dec. 2019.

[36] X. Lu, Y. Chen, M. Fu, and H. Wang, "Multi-objective optimization-based real-time control strategy for battery/ultracapacitor hybrid energy management systems," *IEEE Access*, vol. 7, pp. 11640–11650, 2019.
[37] C. Zhang, A. Vahidi, P. Pisu, X. Li, and K. Tennant, "Role of Terrain preview in energy management of hybrid electric vehicles," *IEEE Trans. Veh. Technol.*, vol. 59, no. 3, pp. 1139–1147, Mar. 2010.
[38] K. W. Chew, C. K. Leong, and B. M. Goi, "Contour data acquisition system for electric vehicle distance estimation method," *Appl. Mech. Mater.*, vols. 479–480, pp. 503–507, Dec. 2013.
[39] E. Coelingh and S. Solyom, "All aboard the robotic road train," *IEEE Spectr.*, vol. 49, no. 11, pp. 34–39, Nov. 2012.
[40] M. Chen and G. A. Rincon-Mora, "Accurate electrical battery model capable of predicting runtime and I–V performance," *IEEE Trans. Energy Convers.*, vol. 21, no. 2, pp. 504–511, Jun. 2006.
[41] A. Shafiei, A. Momeni, and S. S. Williamson, "Battery modeling approaches and management techniques for plug-in hybrid electric vehicles," in *Proc. IEEE Vehicle Power Propuls. Conf.*, Sep. 2011, pp. 1–5.
[42] A. Fotouhi, D. J. Auger, K. Propp, S. Longo, and M. Wild, "A review on electric vehicle battery modelling: From lithium-ion toward Lithium–Sulphur," *Renew. Sustain. Energy Rev.*, vol. 56, pp. 1008–1021, Apr. 2016.
[43] S. Barsali and M. Ceraolo, "Dynamical models of lead-acid batteries: Implementation issues," *IEEE Trans. Energy Convers.*, vol. 17, no. 1, pp. 16–23, Mar. 2002.
[44] T. Huria, M. Ceraolo, J. Gazzarri, and R. Jackey, "High fidelity electrical model with thermal dependence for characterization and simulation of high power lithium battery cells," in *Proc. IEEE Int. Electric Vehicle Conf.*, Greenville, CA, USA, Mar. 2012, pp. 1–8.
[45] P. Sharma and T. S. Bhatti, "A review on electrochemical double-layer capacitors," *Energy Convers. Manage.*, vol. 51, no. 12, pp. 2901–2912, Dec. 2010.
[46] L. Zubieta and R. Bonert, "Characterization of double-layer capacitors for power electronics applications," *IEEE Trans. Ind. Appl.*, vol. 36, no. 1, pp. 199–205, 2000.
[47] N. Devillers, S. Jemei, M.-C. Péra, D. Bienaimé, and F. Gustin, "Review of characterization methods for supercapacitor modelling," *J. Power Sources*, vol. 246, pp. 596–608, Jan. 2014.
[48] M. R. D. Al-Mothafar, "Small-and large-signal modelling of a modular boost-derived DC-DC converter for high-output voltage applicaTIONS," *Int. J. Model. Simul.*, vol. 26, no. 1, pp. 52–60, 2006.
[49] M. A. Abdullah, C. W. Tan, A. H. Yatim, M. Al-Mothafar, and S. M. Radaideh, "Input current control of boost converters using current-mode controller integrated with linear quadratic regulator," *Int. J. Renew. Energy Res.*, vol. 2, pp. 262–268, 2012.
[50] T. Sadeq and C. K. Wai, "Model the DC-DC converter with supercapacitor module based on system identification," in *Proc. IEEE Int. Conf. Autom. Control Intell. Syst. (I2CACIS)*, Jun. 2019, pp. 185–188.
[51] F. Machado, J. P. F. Trovao, and C. H. Antunes, "Effectiveness of supercapacitors in pure electric vehicles using a hybrid Metaheuristic approach," *IEEE Trans. Veh. Technol.*, vol. 65, no. 1, pp. 29–36, Jan. 2016.
[52] D. Maksimovic, A. M. Stankovic, V. J. Thottuvelil, and G. C. Verghese, "Modeling and simulation of power electronic converters," *Proc. IEEE*, vol. 89, no. 6, pp. 898–912, Jun. 2001.
[53] M. A. Abdullah, C. W. Tan, and A. H. M. Yatim, "A simulation study of hybrid wind-ultracapacitor energy conversion system," in *Proc. IEEE Conf. Energy Convers. (CENCON)*, Johor Bahru, Malaysia, Oct. 2014, pp. 265–270.
[54] K. Wipke, "ADVISOR 2.0: A second-generation advanced vehicle simulator for systems analysis," *Naevi*, vol. 98, pp. 3–4, Dec. 1999.
[55] A. Fotouhi, K. Propp, and D. J. Auger, "Electric vehicle battery model identification and state of charge estimation in real world driving cycles," in *Proc. 7th Comput. Sci. Electron. Eng. Conf. (CEEC)*, Colchester, U.K., Sep. 2015, pp. 243–248.
[56] C. K. Wai, Y. Y. Rong, and S. Morris, "Simulation of a distance estimator for battery electric vehicle," *Alexandria Eng. J.*, vol. 54, no. 3, pp. 359–371, Sep. 2015.
[57] A. Bampoulas, A. Giannakis, S. Tsaklidou, and A. Karlis, "Modeling, simulation and performance evaluation of a low-speed battery electric vehicle," in *Proc. 11th Int. Conf. Ecol. Vehicles Renew. Energies (EVER)*, Apr. 2016, pp. 1–8.
[58] B. Sri Kaloko, M. Soebagio, and M. Hery Purnomo, "Design and development of small electric vehicle using MATLAB/Simulink," *Int. J. Comput. Appl.*, vol. 24, no. 6, pp. 19–23, Jun. 2011.
[59] K. Mahmud and G. E. Town, "A review of computer tools for modeling electric vehicle energy requirements and their impact on power distribution networks," *Appl. Energy*, vol. 172, pp. 337–359, 2016.
[60] J. Larminie and J. Lowry, *Electric Vehicle Technology Explained, 2003*. Hoboken, NJ, USA: Wiley, 2003.
[61] M. Ehsani, Y. Gao, and A. Emadi, *Modern Electric, Hybrid Electric, and Fuel Cell Vehicles: Fundamentals, Theory, and Design*, 2nd ed. Boca Raton, FL, USA: CRC Press, 2010.
[62] Q. A. Tarbosh, O. Aydogdu, N. Farah, M. H. N. Talib, A. Salh, N. Cankaya, F. A. Omar, and A. Durdu, "Review and investigation of simplified rules fuzzy logic speed controller of high performance induction motor drives," *IEEE Access*, vol. 8, pp. 49377–49394, 2020.
[63] N. Farah, M. H. N. Talib, N. S. Mohd Shah, Q. Abdullah, Z. Ibrahim, J. B. M. Lazi, and A. Jidin, "A novel self-tuning fuzzy logic controller based induction motor drive system: An experimental approach," *IEEE Access*, vol. 7, pp. 68172–68184, 2019.
[64] K. Boriboonsomsin and M. Barth, "Impacts of road grade on fuel consumption and carbon dioxide emissions evidenced by use of advanced navigation systems," *Transp. Res. Rec., J. Transp. Res. Board*, vol. 2139, no. 1, pp. 21–30, Jan. 2009.
[65] T. Sadeq and C. K. Wai, "Linear quadratic regulator control scheme on hybrid energy storage system," in *Proc. IEEE Int. Conf. Autom. Control Intell. Syst.*, Jun. 2020, pp. 219–223.
[66] A. Wangsupphaphol, N. R. N. Idris, A. Jusoh, and N. D. Muhamad, "Power converter design for electric vehicle applications," *J. Teknol.*, vol. 67, no. 3, pp. 25–31, Mar. 2013.

**TAHA SADEQ** (Member, IEEE) was born in Yemen, in 1985. He received the B.Eng. degree from Omdurman Islamic University, Sudan, in 2009, and the M.Eng. degree in electrical engineering from Universiti Teknologi Malaysia in 2015. He is currently pursuing the Ph.D. degree with Universiti Tunku Abdul Rahman, Sungai Long Campus, Malaysia. His research interests are in hybrid energy storage system, batteries supercapacitors, dc–dc converter, and electric vehicle.

**CHEW KUEW WAI** (Senior Member, IEEE) was born in Kelantan, Malaysia, in 1974. He received the Ph.D. degree in physics from Universiti Malaya, Malaysia. He is currently an Associate Professor with the Department of Electrical and Electronic Engineering, Universiti Tunku Abdul Rahman, Sungai Long Campus, Malaysia. His major field of study is on the lithium-ion batteries and electric vehicles.

**EZRA MORRIS** received the B.Eng. degree from Bharathiar University, India, the M.E. degree from Anna University, India, and the Ph.D. degree from Multimedia University, Malaysia. In 2008, he joined Universiti Tunku Abdul Rahman, Sungai Long Campus (UTAR), Malaysia. Since 2018, he has been the Deputy Director of IPSR UTAR. His research areas include digital signal processing and optimization, using PSO, GA/IGA, and mobile communication.

**QAZWAN A. TARBOSH** (Member, IEEE) was born in Taiz, Yemen. He received the bachelor's degree in electrical and electronic engineering and the master's degree in electrical and electronic engineering from Universiti Tun Hussein Onn Malaysia in 2013 and 2015, respectively, where he is currently pursuing the Ph.D. degree. His research interests in control systems, wireless technology, and antenna filter design.

**ÖMER AYDOĞDU** was born in Konya, Turkey, in 1973. He received the B.S., M.S., and Ph.D. degrees in electrical and electronics engineering from Selçuk University, Konya, in 1995, 1999, and 2006, respectively. He is currently a Professor with Konya Technical University. His research interests include control theory, adaptive control systems, fractional order control, fuzzy logic control and applications, and brushless dc motors and drives.